Diabetic Foot Ulcers Healing Promoted by Novel Glibenclamide-Loaded Micelle Wound Dressing

ABSTRACT: Diabetic foot ulcers (DFU) are chronic wounds, which do not respond to traditional wound treatments. In this work, wound dressings of glibenclamide (GB) incorporated into a novel mixed matrix were fabricated in the aim of accelerating the healing process of diabetic wounds. GB was loaded into different weight ratios of Soluplus® (SP) and polyvinylpyrrolidone (PVP). The developed dressings were characterized in vitro and in vivo, for their ability to promote diabetic wound healing. The particle size was between (1.4-2) µm. The morphology abided by the SP/PVP ratio in the formulated microparticles. Cup/bowl shape, semispherical with corrugated surface, apple shape with smooth surface, concave/star shape, and Irregular corrugated morphology were denoted for GB-SP/PVP1-0, GB-SP/PVP1-1, GB-SP/PVP0-1, GB-SP/PVP1-2, and GB-SP/PVP2-1 formulations, respectively. Glibenclamide was in amorphous form and hydrogen-bonded with the matrix polymers. The GB-SP/PVP0-1 wound dressings showed a burst drug release in about 1 hour due to the hydrophilic nature of PVP. The other GB-SP/PVP formulated polymeric micelles were of sustained release, where GB-SP/PVP2-1 extended the drug release for 48 hours. The MTT assay showed that all GB-SP/PVP dressings have good cytocompatibility, and in consequence, they can be used in further investigations on biomedical applications. In vivo tests on a rat model of a full-thickness wound showed rapid closure, indicating the success of the wound dressings in decreasing inflammation and promoting wound healing without scar formation. Therefore, topical administration of GB-SP/PVP1-0 and GB-SP/PVP2-1 wound dressings has a high potential for the treatment of diabetic wounds in inflammatory and proliferative phases of healing with high bioavailability and fewer systemic adverse effects.

KEYWORDS: diabetic wound dressing; hybrid micelles; soluplus; glibenclamide; electrospraying.

1. INTRODUCTION

The skin is the largest exposed organ of the body which mainly acts as a barrier against the external environment and it accounts for (5-15) % of the total body weight with an area of (1.5-2) m^2 [1]. The skin has great potentials to heal itself after an injury, a cut or a burn. However, in some cases the wounds would not heal as they should, where the wounds seem not to heal in a well-timed manner, compromising the patient health. The wounds that take more than three months to heal are referred to as chronic wounds [2].

Diabetes mellitus (DM) is a group of metabolic disorders, that is mainly characterized by hyperglycemia, as a result of deficiencies in insulin secretion and/or insulin action [3]. Long-term damage, dysfunction, and failure of different organs are related to chronic hyperglycemia of diabetes [3]. According to the World Health Organization (WHO) report, 422 million adults have diabetes with about 20% of them developing diabetic chronic wounds worldwide [4], [5]. Diabetic chronic wounds are classified into three types: foot, venous, and pressure ulcers [6]. Diabetic foot ulcers are chronic, non-healing wounds that generate disruption in the skin with an unfulfilled and prolonged healing process [7]. The global spread of 6.3% diabetic foot ulcers represents a heavy burden on public health [8]. Individuals with chronic wounds and diabetic foot ulcers are at high risk for lower extremity amputation due to the threat of osteomyelitis and/or sepsis as a result of wound infection [7]. In the normal course of wound healing, hemostasis takes place that inspects the blood loss and invasion of microbes to the wounded area, followed and interfered by inflammation as pro-inflammatory cells neutrophils upregulate (initially) and then macrophages ensue to remove detritus and pathogens and releasing growth factors and cytokines [5]. The proliferative phase is characterized by forming of new tissues, new blood vessels (angiogenesis) and extracellular matrix (ECM) deposition to seal the wounded area [5]. The last stage of wound healing process is the remodeling phase, where ECM consists mainly of collagen to increase the tensile strength of the tissue to about 80% of normal tissue and the blood supply to the wounded area is reduced [2]. Diabetes causes a dysfunctional alteration in the healing process where it impairs each phase of wound healing that is hemostasis, inflammation, proliferation and remodeling phase

[2], [5]. The need for novel therapeutic approaches with innovative technology is indispensable to improving the treatment of diabetic wounds. Diabetic wounds are indicated as being in a persistent inflammatory phase characterized by accumulation of pro-inflammatory macrophages, cytokines, and proteases [9]. Mirza et al. [10] found that sustained inflammasome activity in wound macrophages contributes to impaired early healing responses of diabetic wounds which is induced by the activity of the Nod-like receptor protein (NLRP)-3 inflammasome. The topical glibenclamide inhibits the NLRP-3 and reduces the levels of cytokines interleukin (IL)-1β and IL-18 and improved the healing of diabetic wounds, stimulating a switch from proinflammatory to healing associated macrophages phenotypes, and increased levels of prohealing growth factors. The inflammasome may represent a new therapeutic target for improving healing in diabetic wounds. Glibenclamide (GB) was shown to have a high anti-inflammatory action due to the presence of sulfonyl and benzamido groups in its chemical structure that allow for its specific (NLRP)-3 inflammasome inhibitory activity, which is not shared by other sulfonylurea antidiabetics [9], [11]. In addition, glibenclamide inhibits collagenases and participates in controlling MMP activation and collagen degradation [12].

Many studies showed the promising use of glibenclamide as a topical wound treatment to reduce inflammation and stimulate healing of chronic diabetic wounds [13], [14]. Wound dressing is one route of drug delivery systems to treat diabetic foot ulcers. The optimized wound dressing should not only provide a barrier for protection but should also have inherent healing properties, and the ability to release the loaded biomolecules or therapeutics in a time-dependent manner [15]. In this regard, the matrix used to load the therapeutics regulates the release. The hydrophilic polymer polyvinylpyrrolidone (PVP) is used to achieve a burst release. The amphiphilic polymer Soluplus® is of a sustained release. Soluplus® (SP) forms micelles at very low concentrations (7.6 mg/L) in aqueous solutions, which makes it suitable for the topical delivery, where the poorly water soluble drug is captured into the hydrophobic core of these micelles in a supersaturated state [16]. The blend of these two different polymers in different ratios is meant to study their interaction and contribution on the diabetic wounds healing. The combination of the novel technology electrospraying and the repurposed drug glibenclamide loaded into mixed matrix intended to produce glibenclamide-loaded polymeric micelles represent an innovative approach to improve the diabetic wounds healing.

Soluplus for topical application has been reported as thermothickening factor [17], as nanofibers [18], and in the form of hot melt extrudates [19]. Soluplus as microparticle micelles has never been used in skin delivery. Also, the GB-loaded SP/PVP micelles in different polymers ratios and their effect on diabetic wound efficacy has never been studied. The present work develops microparticle micelles, GB-loaded SP/PVP by electrospraying for the purpose of dressing diabetic wounds. Topical application of SP/PVP polymeric micelles with GB was hypothesized to support re-epithelialization and augment cutaneous wound closure in a diabetic animal model. The developed dressings were characterized in vitro for pharmaceutical attributes including morphology, physical and chemical composition, drug release behaviors, in vitro cytotoxicity and in vivo tests for their ability to promote diabetic wound healing.

2. Material and Methods:

Glibenclamide powder (GB) was purchased from Shanghai Ruizheng Chemical Technology Co., Ltd (Shanghai, China). Polyvinylpyrrolidone (PVP) K30 (MW= 30,000), N-Cetyl-N,N,N-Trimethyl ammonium bromide (Hexadecyltrimethyl ammonium bromide) LR (MW= 364.45), and Chloroform were obtained from Central Drug House (P) Ltd. (New Delhi, India). Soluplus® (SP) (MW= 118000 g/mol) was purchased from BASF SE (Ludwigshafen, Germany). Methanol A.R. from Chem-Lab NV (Zedelgem, Belgium), Ethanol absolute anhydrous from Carlo Erba Reagents S.A.S (Val de Reuil Cedex, France), and Acetone from Alpha Chemika (India). Methylene Chloride extra pure and Sodium hydroxide purified pellets LR (MW= 40 g/mol) were acquired from Thomas Baker Chemicals Pvt. Ltd. (Mumbai, India) and Potassium dihydrogen orthophosphate Hi-LR (MW= 136.09) from Himedia Laboratories Pvt. Ltd. (Mumbai, India). All chemicals and reagents used were of analytical grade and were used as received without any further purification.

2.1 Solutions and Particles Preparation

A solution with concentration of 5 % (w/v) at drug/ polymer ratio (1/4 w/w) were prepared by dissolving GB in solvents mixture of ethanol and chloroform (3/2 v/v); thoroughly mixed by a magnetic stirrer for about an hour to make sure it completely dissolved. Then, the polymers (SP/PVP) in the ratios (1/0, 0/1, 1/1, 1/2, and 2/1 w/w) were added and stirred for another hour. A horizontal single nozzle electrospraying setup was utilized to generate microparticles of GB-SP/PVP. The solution was loaded up into a plastic syringe 5 ml with 25G stainless

steel needle, the syringe was placed onto a syringe pump (Model no.300, New Era Pump Systems, USA) with fixed flowrate at 1 mL/hr. A high voltage was exerted on the stainless steel nozzle by a high voltage power supply (HV350REG Positive, Information Unlimited, USA). The voltage ranged between (8-9 kV). The distance between the needle tip and the collector plate was constant at 8 cm.

2.2 Characterization of Particle Size and Morphology

The particle size and morphology were characterized through a field emission scanning electron microscope (FESEM) (Mira3, Tescan, France). The samples were prepared by taking a thin layer of particles, sputtered with gold and mounted on metallic stubs with double sided carbon tape and were viewed at an accelerating voltage of 15 kV. The obtained images were utilized to determine the mean diameter of the nanoparticles.

2.3 X-Ray Powder Diffraction (XRPD)

The diffraction patterns of the raw GB, PVP and the optimized sample of GB loaded PVP nanoparticles were analyzed using the PANalytical X'Pert PROMPD system (PW3040/60, Philips, the Netherlands) utilizing Cu Kα radiation (λ= 1.542 Å). The measurements were carried out in the reflection mode 2θ in the range (10˚- 80˚) scanned at 40 kV and 30 mA. The scanning rate was 4 min^{-1}.

2.4 Fourier Transform Infrared Spectroscopy (FTIR)

The type of interaction between the drug and the polymer was investigated by using FTIR. Samples were of raw GB, PVP powder, a physical mixture of GB-PVP powder and optimized GB-PVP nanoparticles. A sample of 2 mg was mixed with 10 mg of potassium bromide, compressed into a disk and placed in the device (8400S, Shimadzu, Japan). The scanning range is (4000- 400) cm^{-1}.

2.5 In Vitro Release Study

The release of GB from the wound dressings was studied by enclosing the wound dressings in a nylon mesh and separately immersing them in 100 ml release media of phosphate buffer pH 7.4 containing CTAB 0.1% (w/v) to assure the sink conditions under magnetic stirring at 100 rpm and 37 ºC. A 2 mL sampling at predetermined time intervals with replacement was conducted. Samples were filtered using 0.45 µm syringe filters and analyzed spectrophotometrically (Cary 100, Varian, USA) at the selected λ_{max}.

2.6 Cell Culture

The mouse embryo fibroblast (NIH/3T3) cell line was acquired from American Type Culture Collection (ATCC). Cells were cultured in Dulbecco's modified Eagle medium (DMEM, Invitrogen, UK) supplemented with 10% Fetal bovine serum (FBS, Gibco) and 1% penicillin/streptomycin in a 5% CO2 humidified air incubator, kept at 37°C. When the cells attained 80% of confluence they were washed with PBS and trypsinized with 0.25% Trypsin-EDTA for passaging and seeding each time. The confluent cells were employed in cytotoxicity tests.

2.6.1 Cell viability assay

The in vitro cell viability of the GB-loaded SP/PVP micelles was assessed by methylthiazolydiphenyl-tetrazolium Bromide (MTT) assay [20], [21]**.** MTT assays were implemented in 96-well plates. About 105 NIH/3T3 cells per well were seeded onto the 2 hours UV sterilized polymers and incubated for 3 days. The measurement of cell viability was done by determining mitochondrial NADH/NADHP–dependent dehydrogenase activity, which caused the cellular conversion of the 3-(4, 5-dimethylthiazol-2-gl)-5-(3-carboxymethoxylphenyl)-2-(4-sulfophenyl-2H) tetrazolium salt into a soluble formazan dye. Three days later, supernatants were taken off, and 10 µl 3-(4, 5-dimethylthiazol-2yl)-2,5-diphenyl-2H-tetrazolium-bromide (MTT- 5mg/ml- Sigma) solution was put in to each well. After incubation at 37°C for 3.5 hours, these were stored in a dark humidified atmosphere of 5% CO_2 in air. The active cells absorbed MTT and degraded in the mitochondria to an insoluble purple formazan granule [20]. Next, supernatant was eliminated, and the precipitated formazan was dissolved in 100 µL dimethyl sulfoxide per well, the absorbance was measured at a wavelength of 570 nm using a Kayto RT-2100C microplate reader to determine optical density of the solution (Rayto, China).

2.7 In Vivo Wound Healing Experiments

Fifty male and female Sprague-Dawley rats aged 8-9 weeks, weighing 300-350 gram were obtained from Al-Nahrain University Biotechnology Research Center. The rats were housed under suitable environmental conditions of temperature (20-25)˚C, humidity (40-60) %, and light (12 hours light/dark regime). They were held on a standard rodent pellet diet, with tap water freely available.

2.7.1 Experimental Design of Wound Healing Experiment

To induce type-1 Diabetes mellitus in rats, a single dose of 60 mg/kg streptozotocin (STZ) was injected intraperitoneally, after overnight fasting. The dose was prepared in sodium citrate buffer (0.1 mol/L, pH 4.5) immediately before using. The diabetic status was confirmed 72 hours following STZ injections by measuring the blood glucose level collected from tail vein with a glucometer (AccuChek, Roche Diagnostics, Indianapolis, IN). Rats showing blood glucose levels more than 300 mg/dl were deemed diabetic and involved in the experiment [22], [23]. The animals were maintained for 10 days after STZ administration to initiate a chronic hyperglycemic state [23]. All animals were anesthetized by intraperitoneal injection with Ketamin/xylazine (40–4 mg/kg) and then the dorsal hair of diabetic rats was entirely shaved and the skin was disinfected with povidone-iodine. To create a full-thickness wound to the deep fascia, the skin was punched with a sterile 8 mm biopsy punch (Kai Medical, BP-80F Japan) [24]. The rats were separated into five groups, each of 10 animals: 1) control group of diabetic wound with no treatment, 2) pure SP/PVP2-1 group treated with pure SP/PVP (2/1 w/w) dressings only without active drug, 3) GB-SP/PVP1-1 group treated with GB-loaded SP/PVP (1/1 w/w) dressings, 4) GB-SP/PVP1-0 group treated with GB-loaded SP/PVP (1/0 w/w) dressings, and 5) GB-SP/PVP2-1 group treated with GB-loaded SP/PVP (2/1 w/w) micelles dressings. The dressing was applied directly to the wounded area and fixed by using a surgical tape. No dressings were changed and no other topical medication was administered, all over the in vivo experiment. The wound area was assessed for all groups on days 0, 3, 7 and 14 by photographing the wound area. The wound closure percentage was calculated by using the following equation:

$$\text{Wound closure percentage} = \frac{A_0 - A_n}{A_n} \times 100\% \qquad (3.4)$$

where A_0 and A_n are the initial wound area at day 0 and the wound area at the day of measurement, respectively.

2.8 Statistical Analysis

The results of the experiments were expressed as a mean value ± standard deviation (SD). The data were analyzed using one-way ANOVA by Dunnettis *t*-test. The interactions between the different groups in MTT test, and animal test were tested using analysis of variance (ANOVA) with 95% confidence interval and Bonferroni's post hoc test. The results were expressed as mean ± standard error mean. The values would be significant if $p<0.05$, and non-significant if $P > 0.05$. The analysis was performed with GraphPad Prism 7.0 software (GraphPad, La Jolla, CA, USA).

3. RESULTS and DISCUSSION

Diabetic wounds and diabetic foot ulcers treated with traditional wound dressings are not responding to treatment, depicting the need for new fabrication methods. The adaptation of a polymer to the type of injury to be healed will serve the optimization of properties of the therapeutic delivered by such a carrier. The GB-loaded polymeric micelles dressings are one route of methods, where the unique properties of each polymer govern the release kinetics of the therapeutics and contribute to accelerating the healing process of diabetic wounds.

3.1 Particle Size and Morphology

The electrospraying process was used to generate the GB-SP/PVP microparticles. The associated different process and formulation parameters made this technology feasible to produce versatile particle size and shape via the required criteria of the application. The particle size was 2 ± 0.58, 1.8 ± 0.57, 1.4 ± 0.27, 1.7 ± 0.45, and 1.9 ± 0.64 µm for GB-SP/PVP1-0, GB-SP/PVP1-1, GB-SP/PVP1-2, GB-SP/PVP0-1, and GB-SP/PVP2-1, respectively. The morphology of the mixed polymers micelles is shown in Fig. 1. The GB-SP/PVP1-0 microparticles comprising SP only showed the largest size which is comparable to the ratio of SP/PVP (2/1 w/w) that exhibit the highest size distribution. It is a consequence of the high molecular weight of SP. The morphology is strictly related to the

SP/PVP ratio in the formulated microparticles. The GB-SP/PVP1-0 microparticles incorporated with SP only were of cup/bowel shape, while GB-SP/PVP1-1 of the same amount of PVP and SP in the matrix delivered microparticles of semispherical with corrugated surface morphology. The GB-SP/PVP0-1 formulations of GB loaded PVP only matrix exhibited an apple shape with a smooth surface. GB-SP/PVP1-2 micelles of SP/PVP (1/2 w/w) ratio were of concave/star shape particles. Irregular corrugated morphology denoted by GB-SP/PVP2-1 formulation. This varied morphology of GB-SP/PVP micelles indicates strongly the interaction between the polymers with the dispersed drug within. The different morphology is responsible for different drug releases and could be related to the absorption route in the different cells. Electrospraying produced different size and shape of particles depending on the used polymers and via process and formulation parameters. The ability in shaping the particles with the desired morphology is a unique feature of electrospraying in comparison with other processes.

3.2 XRPD of The Wound Dressings

The XRPD diffraction patterns of GB, SP, PVP and GB-SP/PVP in the selected ratios are depicted in Fig. 2. All the GB-SP/PVP microparticle diffractograms exhibited an amorphous state indicating the absence of the crystalline GB molecules and the dispersion of them within the SP/PVP matrix and the blended of the polymers with each other uniformly.

3.3 Wound Dressings Composition

The FTIR was utilized to analyze the molecular contents of the microparticles wound dressings and it was verified that GB was loaded successfully into the SP/PVP microparticles. The molecular structures of pure GB, SP, PVP, and GB-SP/PVP in the selected polymers ratios are shown in Fig. 3 . GB showed characteristics peaks at 3369 and 3316 cm^{-1} corresponded to the amide stretching bands, C=O stretching vibration at 1714 cm^{-1}, HN-C=O stretching at 1620 cm^{-1}, symmetric and asymmetric S=O2 stretching at 1344 and 1159 cm^{-1}, respectively [25], [26]. Pure SP showed aromatic C-H stretching at 2928 cm^{-1}, =C-O-C stretching at 1737 cm^{-1}, C=O stretching for tertiary amide at 1638 cm-1, C-O-C stretching at 1472 cm^{-1} and C-O stretching at 1242 cm^{-1} [27], [28]. Peaks for pure PVP were detected at 3449 cm^{-1} corresponding to O-H bending, C-H stretching band at 2955 cm^{-1}, the characteristic and the most intensive absorption band amide C=O stretching vibration at 1668 cm^{-1} [29]. The C-H bending band at 1373 cm^{-1}, characteristic absorption band of C–N stretching at 1284 cm^{-1}, and CH_2 twist bands at 1228 and 1170 cm^{-1} [30], [31]. The spectrum of all the GB-SP/PVP micelles wound dressings showed original peaks at 3369 and 3316 cm^{-1}, which are referred to GB. For GB-SP/PVP1-0 formulation, which composes of SP only, peaks at 1737 (shifted to 1736), 1638 (shifted to 1636), and 1472 (shifted to 1477) cm^{-1} are assigned to SP. For GB-SP/PVP0-1, comprises of PVP only, peaks at 1668 (shifted to 1667), 1377 (shifted to 1371), and 1284 (shifted to 1286) cm^{-1} are attributed to PVP. In the other samples formulated with different SP/PVP ratios, peaks at 1668 and 1371 cm^{-1} are assigned to PVP, and peaks at 1737 and 1242 cm^{-1} are attributed to SP. According to these results, successful drug encapsulation and formulation were achieved with no polymer–drug interaction.

3.4 In Vitro Drug Release

Analysis was performed to investigate the in vitro drug release of glibenclamide from GB-SP/PVP2-1, GB-SP/PVP1-1, GB-SP/PVP1-2, GB-SP/PVP1-0, and GB-SP/PVP0-1 in phosphate buffer saline of pH 7.4 at a temperature of 37 ºC to simulate the physiological environments of living organisms. The release profiles are shown in Fig. 4. The GB-SP/PVP micelles were of high %EE (> 98%). The GB-loaded PVP microparticles (GB-SP/PVP0-1) wound dressings exhibited a burst drug release in nearly one hour due to the PVP inherited property of hydrophilicity. Further, the GB embedded in SP/PVP micelles with various polymer ratios were of a sustained drug release across 48 hours, and this is referred to the amphipathic nature of SP. The GB-SP/PVP1-0 dressings demonstrated a burst release for 4 hours followed by a sustained release of GB for 36 hours. The micelles' formation kept the GB in a supersaturated state as the drug was captured within the hydrophobic core. The dressings of GB-SP/PVP1-1 continuously released GB for 12 hours, with an initial burst for 2 hours (> 40 µg/mL), followed by a steady increase till the peak at 12 hours (50 µg/mL), after which the concentration gradually decreased. The presence of PVP increases the GB release which, was maintained for an extended period due to the solubilization effect of SP, which is consistent with [32]. The increase in the SP/PVP ratio as in the dressings of GB-SP/PVP2-1 slows the GB release to deliver (~ 30 µg/mL) in 24 hours, while a peak (> 45 µg/mL) at 48 hours was detected. The observation of contradictory situation with the dressings of GB-SP/PVP1-2, where the lower ratio of SP/PVP showed a burst release of 70 % for 8 hours then the release was

suppressed. These results indicate that the addition of PVP to the SP solution led to a structural change in the micelles of Soluplus [16]. When SP is below the CMC, it aggregates with the hydrophobic region of PVP, and when the SP concentration exceeds the CMC, the hydrophobic part of SP self-assembled to form micelles, PVP which is attached to SP by hydrophobic interaction, now aggregated at the hydrophilic-hydrophobic boundary of the micelles [16]. When the SP concentration is higher than PVP, the hydrophobic group is larger than the hydrophilic part, and the slow drug release is due to the strong hydrophobic interaction between GB and the core of the micelles. The increase in PVP concentration on the count of SP creates a larger hydrophilic region compromising the GB hydrophobic interaction with the core of the micelles and promoting the drug release, but sooner crystallization took place, as in the case of GB-SP/PVP1-2 dressings. The different drug behaviors of GB marked by the release profiles of the wound dressings assume varied biological effects, as were observed in the healing of diabetic wounds in rats.

3.5 Evaluation of Cell Viability

The investigation of cell viability to perform a cytotoxicity test is essential to evaluate the potential of the GB-loaded SP/PVP micelles as a wound dressing. The MTT assay showed that pure SP/PVP and GB-SP/PVP showed negative cytotoxicity in comparison to the control group at 72 hour (Fig. 5). So, these dressings can be safely employed for animal tests and the biocompatibility test confirmed that all GB-loaded micelles dressings retain good cytocompatibility and in consequence they can be used in further investigations on biomedical applications.

3.6 Wound Healing Ability Assessment

Chronic wound healing efficiency of GB-loaded SP/PVP polymeric micelles was evaluated via an in vivo full-thickness diabetic wound model. The chronic wound model was performed by the STZ-induced wound model [33], as these induced diabetic wounds showed persistent inflammation and significantly restrains re-epithelializatoin and wound closure [34]. The wound images of an animal of each group are depicted in (Fig. 6 a): (A) control group, (B) Pure SP/PVP2-1 micelles group, (C) GB-SP/PVP1-1 group, (D) GB-SP/PVP1-0 group, and (E) GB-SP/PVP2-1 group, on days 0, 3, 7, and 14, succeeding wound creation. No evident signs of infection, like redness or swelling, were existing in either treatment group throughout the experimental period. There was no significant difference in the wound appearance between the treated and the untreated rats on the first three days. However, on day 7, The rats in groups C, D, and E showed faster-wound closure compared to group B of the pure SP/PVP micelles and the control group. On day 14, the last day of the in vivo experiment, all the animal groups treated with GB-loaded dressings showed nearly complete wound healing compared to the control group. Also, the hair follicles establishment was noticed merely with groups C, D, and E. As GB-SP/PVP1-0 and GB-SP/PVP2-1 micelles, groups D and E exhibited quicker wound healing on days 7 and 14 with no scar formation. These results are consistent with [13], where topical GB application stimulates RIP140 protein degradation in macrophages, elevating M2 (anti-inflammatory) markers and decreasing M1 (inflammatory) markers in wound tissues, thereby contributing to anti-inflammation and so promoting diabetic wound healing. During the healing period, differences in wound closure between all the experimental groups were observed (Fig. 6 b). On day 3 post-treatment, wounds treated by the GB-SP/PVP1-1 ($P < 0.001$) dressings showed a significantly higher percentage wound closure compared to GB-SP/PVP2-1 ($P < 0.01$), GB-SP/PVP1-0 ($P < 0.01$), pure SP/PVP2-1($P < 0.05$), and control group. Where GB-SP/PVP1-1 showed the most decrease in wound area of 63.4 ± 5.1%, in comparison to 69.7 ± 1.5 %, 74.2 ± 3.3, 87.3 ± 4.5 %, 89.9 ± 3.2 of GB-SP/PVP1-0, GB-SP/PVP2-1, pure SP/PVP2-1, and control group, respectively. This wound contraction could be due to the burst and continuous release of GB from the SP/PVP1-1 micelles providing a high GB concentration that speeds the wound closure. A different path was demonstrated on the 7th day, where the GB-SP/PVP2-1 and GB-SP/PVP1-0 micelles showed the lowest wound area of 37.8 ± 2.4 % and 40.4 ± 2.1% ($P < 0.01$), respectively, while the wounds treated with GB-SP/PVP1-1 were of 45.1 ± 2.3 % ($P < 0.01$) compared to 56.5 ± 1.7 % and 60.2 ± 4.2 % ($P < 0.05$) of pure SP/PVP2-1 micelles and control group, respectively. The SP/PVP2-1 micelles enable the sustained release of GB, which provides more regulated concentrations of the drug into the wounded area than the decreased release of GB-SP/PVP1-1 dressings after 12 hours of treatment, which significantly participate in promoting the healing process. At the end of the experiment, on day 14, the means of the wound area were 6.3 ± 1.4 %, 8 ± 3.2 5, 10.2 ± 1.1 %, 13.7 ± 4.9 %, 21.3 ± 3.2 % of GB-SP/PVP2-1, GB-SP/PVP1-0, GB-SP/PVP1-1, pure SP/PVP2-1, and control group, respectively, with no statistical difference ($P < 0.05$).

4. CONCLUSION

The GB-loaded different weight ratios SP/PVP microparticles were generated via electrospraying, intended for dressing diabetic foot ulcers. The GB-SP/PVP formulations showed diverse particle sizes and morphologies governed by the SP/PVP weight ratios. It was confirmed by the XRPD, FTIR, and %EE tests that GB was encapsulated successfully into the SP/PVP microparticles. The GB embedded in SP/PVP micelles with various polymer ratios showed a sustained drug release over 48 hours, which is attributed to the amphipathic nature of SP. The results indicate that the addition of PVP to the SP solution led to a structural change in the micelles of Soluplus. The GB-loaded SP/PVP wound dressings showed no cytotoxicity effect on the mouse embryo fibroblast (NIH/3T3) cell. The in vivo full-thickness diabetic wound model in rats demonstrated fast wound closure for those treated with the GB-SP/PVP wound dressings, specifically the groups treated with GB-SP/PVP1-0 and GB-SP/PVP2-1 formulations. The high anti-inflammatory glibenclamide promotes diabetic wound healing governed by the designed matrix polymers.

Ethical Approval

The permission for the animal experiments was granted by the Scientific Board and the Scientific Research Ethic Board of the Biotechnology Research Center at Al-Nahrain University.

COMPETING INTERESTS

Authors have declared that no competing interests exist.

REFERENCES

[1] P. Zhou, H. Zhou, J. Shu, S. Fu, and Z. Yang, “Skin wound healing promoted by novel curcumin-loaded micelle hydrogel,” *Ann. Transl. Med.*, vol. 9, no. 14, pp. 1152–1152, 2021, doi: 10.21037/atm-21-2872.

[2] S. Saghazadeh *et al.*, “Drug delivery systems and materials for wound healing applications,” *Adv. Drug Deliv. Rev.*, vol. 127, pp. 138–166, 2018, doi: 10.1016/j.addr.2018.04.008.

[3] A. D. Association, “Diagnosis and Classification of Diabetes Mellitus,” *Diabetes Care*, vol. 37, no. Supplement 1, pp. S81–S90, Jan. 2014, doi: 10.2337/DC14-S081.

[4] WHO Global Report on Diabetes, “Global Report on Diabetes,” 2016. Accessed: Nov. 19, 2021. [Online]. Available: https://www.who.int/publications/i/item/9789241565257.

[5] S. Patel, S. Srivastava, M. R. Singh, and D. Singh, “Mechanistic insight into diabetic wounds: Pathogenesis, molecular targets and treatment strategies to pace wound healing,” *Biomed. Pharmacother.*, vol. 112, no. October 2018, p. 108615, 2019, doi: 10.1016/j.biopha.2019.108615.

[6] A. R. Siddiqui and J. M. Bernstein, “Chronic wound infection: Facts and controversies,” *Clin. Dermatol.*, vol. 28, no. 5, pp. 519–526, Sep. 2010, doi: 10.1016/J.CLINDERMATOL.2010.03.009.

[7] E. Gianino, C. Miller, and J. Gilmore, “Smart wound dressings for diabetic chronic wounds,” *Bioengineering*, vol. 5, no. 3, 2018, doi: 10.3390/bioengineering5030051.

[8] P. Zhang, J. Lu, Y. Jing, S. Tang, D. Zhu, and Y. Bi, “Global epidemiology of diabetic foot ulceration: a systematic review and meta-analysis†,” *Ann. Med.*, vol. 49, no. 2, pp. 106–116, Feb. 2017, doi: http://dx.doi.org/10.1080/07853890.2016.1231932.

[9] J. J. Salazar, W. J. Ennis, and T. J. Koh, “Diabetes medications: Impact on inflammation and wound healing,” *J. Diabetes Complications*, vol. 30, no. 4, pp. 746–752, 2016, doi: 10.1016/j.jdiacomp.2015.12.017.

[10] R. E. Mirza, M. M. Fang, E. M. Weinheimer-Haus, W. J. Ennis, and T. J. Koh, “Sustained inflammasome activity in macrophages impairs wound healing in type 2 diabetic humans and mice,” *Diabetes*, vol. 63, no. 3, pp. 1103–1114, 2014, doi: 10.2337/db13-0927.

[11] M. Lamkanfi *et al.*, “Glyburide inhibits the Cryopyrin/Nalp3 inflammasome,” *J. Cell Biol.*, vol. 187, no. 1, pp. 61–70, 2009, doi: 10.1083/jcb.200903124.

[12] V. L. Bodiga *et al.*, “In vitro biological evaluation of glyburide as potential inhibitor of collagenases,” *Int. J. Biol. Macromol.*, vol. 70, pp. 187–192, 2014, doi: 10.1016/j.ijbiomac.2014.06.054.

[13] Y. W. Lin, P. S. Liu, K. A. Pook, and L. N. Wei, “Glyburide and retinoic acid synergize to promote wound healing by anti-inflammation and RIP140 degradation,” *Sci. Rep.*, vol. 8, no. 1, pp. 1–8, 2018, doi: 10.1038/s41598-017-18785-x.

[14] M. E. Cam *et al.*, “Accelerated diabetic wound healing by topical application of combination oral antidiabetic agents-loaded nanofibrous scaffolds: An in vitro and in vivo evaluation study,” *Mater. Sci. Eng. C*, vol. 119, p. 111586, 2021, doi: 10.1016/j.msec.2020.111586.

[15] D. R. Madhukiran, A. Jha, M. Kumar, G. Ajmal, G. V. Bonde, and B. Mishra, “Electrospun nanofiber-based drug delivery platform: advances in diabetic foot ulcer management,” *Expert Opin. Drug Deliv.*, vol. 18, no. 1, pp. 25–42, 2021, doi: 10.1080/17425247.2021.1823966.

[16] C. Zhu *et al.*, “Supersaturated polymeric micelles for oral silybin delivery: the role of the Soluplus–PVPVA complex,” *Acta Pharm. Sin. B*, vol. 9, no. 1, pp. 107–117, 2019, doi: 10.1016/j.apsb.2018.09.004.

[17] I. Salah, M. A. Shamat, and M. T. Cook, “Soluplus solutions as thermothickening materials for topical drug delivery,” *J. Appl. Polym. Sci.*, vol. 136, no. 1, pp. 1–9, 2019, doi: 10.1002/app.46915.

[18] U. Paaver *et al.*, “Soluplus graft copolymer: Potential novel carrier polymer in electrospinning of nanofibrous drug delivery systems for wound therapy,” *Biomed Res. Int.*, vol. 2014, pp. 14–18, 2014, doi: 10.1155/2014/789765.

[19] M. Nasr, H. Karandikar, R. T. A. Abdel-Aziz, N. Moftah, and A. Paradkar, “Novel nicotinamide skin-adhesive hot melt extrudates for treatment of acne,” *Expert Opin. Drug Deliv.*, vol. 15, no. 12, pp. 1165–1173, 2018, doi: 10.1080/17425247.2018.1546287.

[20] T. Mosmann, “Rapid colorimetric assay for cellular growth and survival: Application to proliferation and cytotoxicity assays,” *J. Immunol. Methods*, vol. 65, no. 1–2, pp. 55–63, Dec. 1983, doi: 10.1016/0022-1759(83)90303-4.

[21] E. Grela, J. Kozłowska, and A. Grabowiecka, “Current methodology of MTT assay in bacteria – A review,” *Acta Histochem.*, vol. 120, no. 4, pp. 303–311, 2018, doi: 10.1016/j.acthis.2018.03.007.

[22] A. Schindl, M. Schindl, H. Pernerstorfer-Schön, K. Kerschan, R. Knobler, and L. Schindl, “Diabetic neuropathic foot ulcer: Successful treatment by low-intensity laser therapy,” *Dermatology*, vol. 198, no. 3, pp. 314–316, 1999, doi: 10.1159/000018140.

[23] C. R. Tim *et al.*, “Mitochondrial dynamics (fission and fusion) and collagen production in a rat model of diabetic wound healing treated by photobiomodulation: comparison of 904 nm laser and 850 nm light-emitting diode (LED),” *J. Photochem. Photobiol. B Biol.*, pp. 41–47, 2019, doi: 10.1016/j.jphotobiol.2018.07.032.Mitochondrial.

[24] S. L. Levengood, A. E. Erickson, F. chien Chang, and M. Zhang, “Chitosan-poly(caprolactone) nanofibers for skin repair,” *J. Mater. Chem. B*, vol. 5, no. 9, pp. 1822–1833, 2017, doi: 10.1039/C6TB03223K.

[25] P. G. Takla, “Glibenclamide,” in *Analytical Profiles of Drug Substances*, vol. 10, 1981, pp. 337–355.

[26] Y. Wang *et al.*, “The role of particle size of glyburide crystals in improving its oral absorption,” *Drug Deliv. Transl. Res.*, vol. 7, no. 3, pp. 428–438, 2017, doi: 10.1007/s13346-017-0378-3.

[27] P. Liu *et al.*, “Soluplus-mediated diosgenin amorphous solid dispersion with high solubility and high stability: Development, characterization and oral bioavailability,” *Drug Des. Devel. Ther.*, vol. 14, pp. 2959–2975, 2020, doi: 10.2147/DDDT.S253405.

[28] A. Homayouni, F. Sadeghi, A. Nokhodchi, J. Varshosaz, and H. A. Garekani, “Preparation and

characterization of celecoxib dispersions in soluplus®: Comparison of spray drying and conventional methods," *Iran. J. Pharm. Res.*, vol. 14, no. 1, pp. 35–50, 2015, doi: 10.22037/ijpr.2015.1621.

[29] L. Cui, Z. P. Liu, D. G. Yu, S. P. Zhang, S. W. A. Bligh, and N. Zhao, "Electrosprayed core-shell nanoparticles of PVP and shellac for furnishing biphasic controlled release of ferulic acid," *Colloid Polym. Sci.*, vol. 292, no. 9, pp. 2089–2096, 2014, doi: 10.1007/s00396-014-3226-8.

[30] G. M. Kim, K. H. T. Le, S. M. Giannitelli, Y. J. Lee, A. Rainer, and M. Trombetta, "Electrospinning of PCL/PVP blends for tissue engineering scaffolds," *J. Mater. Sci. Mater. Med. 2013 246*, vol. 24, no. 6, pp. 1425–1442, Mar. 2013, doi: 10.1007/S10856-013-4893-6.

[31] J. C. Wang, H. Zheng, M. W. Chang, Z. Ahmad, and J. S. Li, "Preparation of active 3D film patches via aligned fiber electrohydrodynamic (EHD) printing," *Sci. Rep.*, vol. 7, Mar. 2017, doi: 10.1038/SREP43924.

[32] K. Punčochová *et al.*, "The Combined Use of Imaging Approaches to Assess Drug Release from Multicomponent Solid Dispersions," *Pharm. Res.*, vol. 34, no. 5, pp. 990–1001, 2017, doi: 10.1007/s11095-016-2018-x.

[33] C. H. Lee *et al.*, "Enhancement of diabetic wound repair using biodegradable nanofibrous metformin-eluting membranes: In vitro and in vivo," *ACS Appl. Mater. Interfaces*, vol. 6, no. 6, pp. 3979–3986, 2014, doi: 10.1021/am405329g.

[34] J. G. Merrell, S. W. McLaughlin, L. Tie, C. T. Laurencin, A. F. Chen, and L. S. Nair, "Curcumin-loaded poly(ε-caprolactone) nanofibres: Diabetic wound dressing with anti-oxidant and anti-inflammatory properties," *Clin. Exp. Pharmacol. Physiol.*, vol. 36, no. 12, pp. 1149–1156, Dec. 2009, doi: 10.1111/J.1440-1681.2009.05216.X.

FIGURES

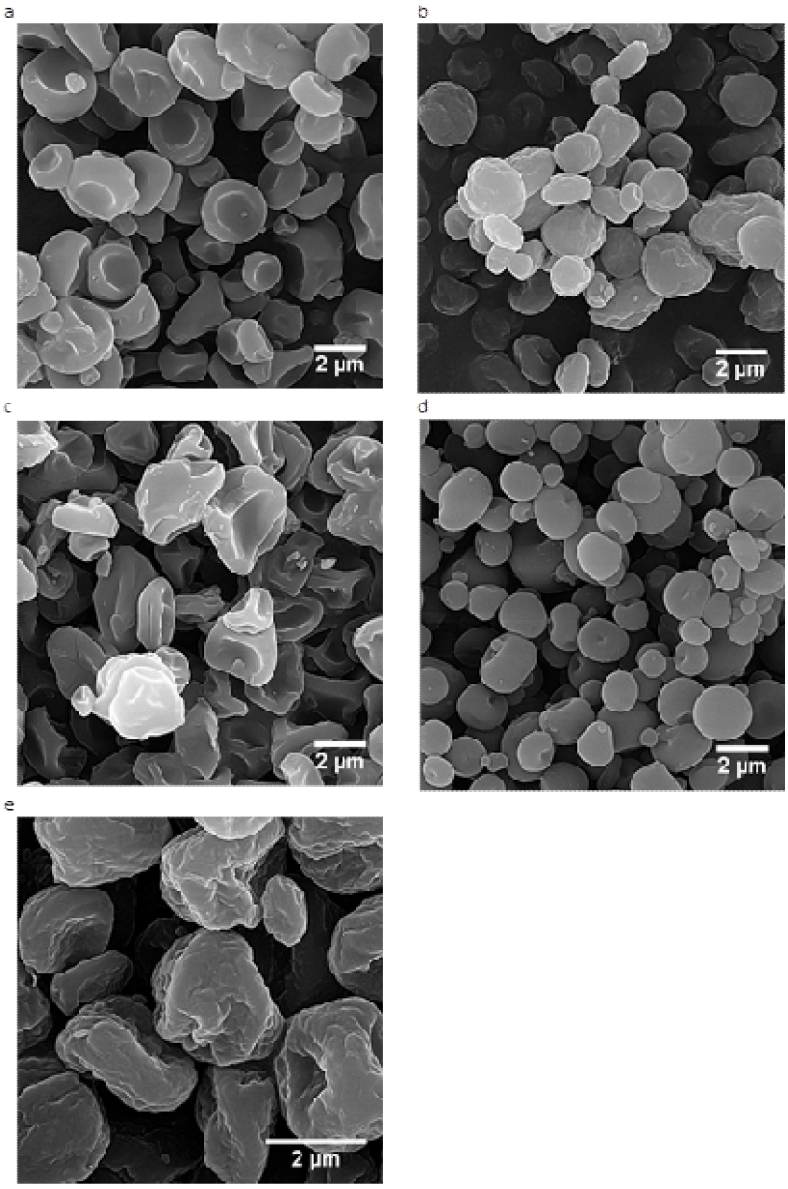

Fig. 1. FESEM images of GB-SP/PVP micelles dressings: (a) GB-SP/PVP1-0, (b) GB-SP/PVP1-1, (c) GB-SP/PVP0-1, (d) GB-SP/PVP1-2, and (e) GB-SP/PVP2-1.

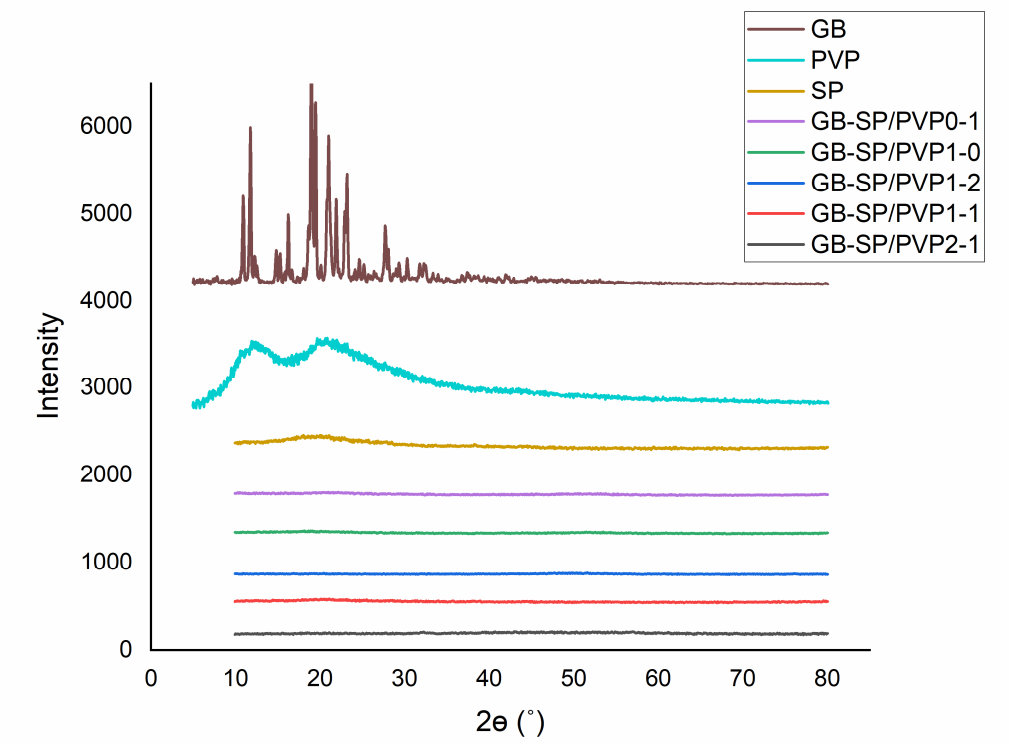

Fig. 2. The XRPD diffractograms of pure GB, PVP powder, SP powder, and GB-loaded different weight ratios SP/PVP wound dressings.

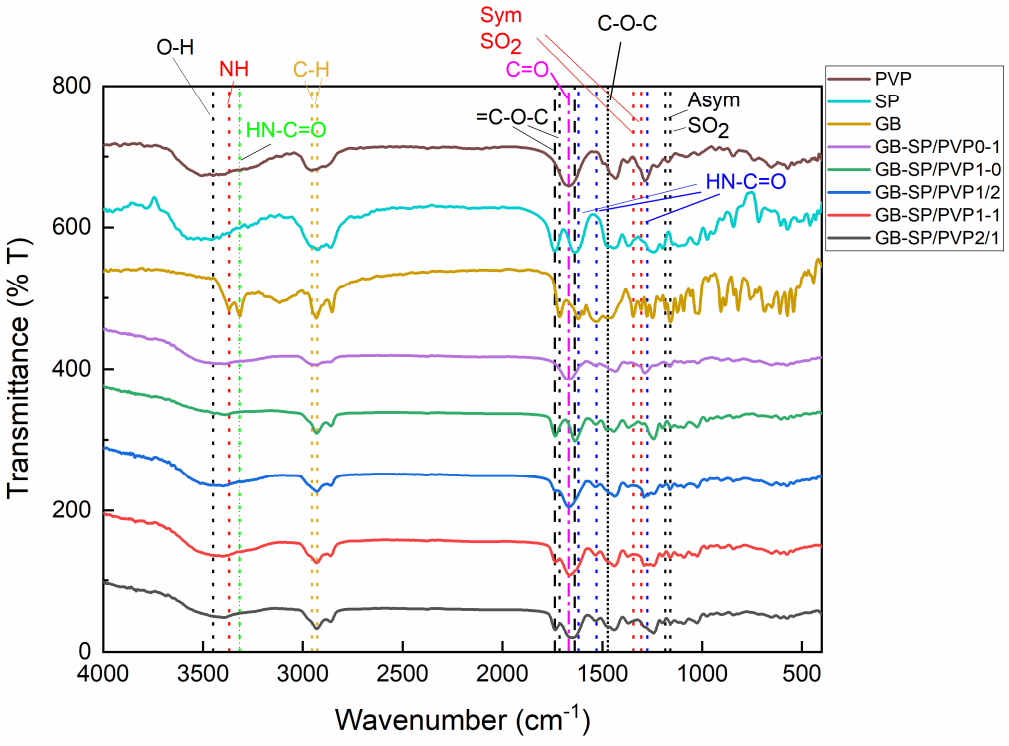

Fig. 3. FTIR spectra of pure GB, PVP powder, SP powder, and GB-loaded different weigh ratios SP/PVP wound dressings.

a

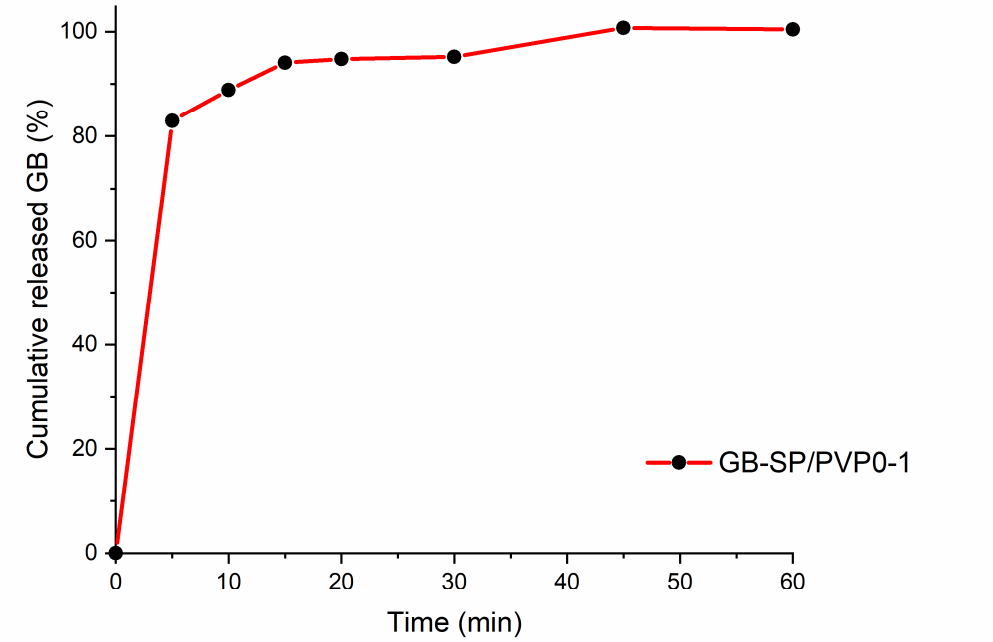
Cumulative released GB (%)
Time (min)
GB-SP/PVP0-1
0
20
40
60
80
100
0
10
20
30
40
50
60

b

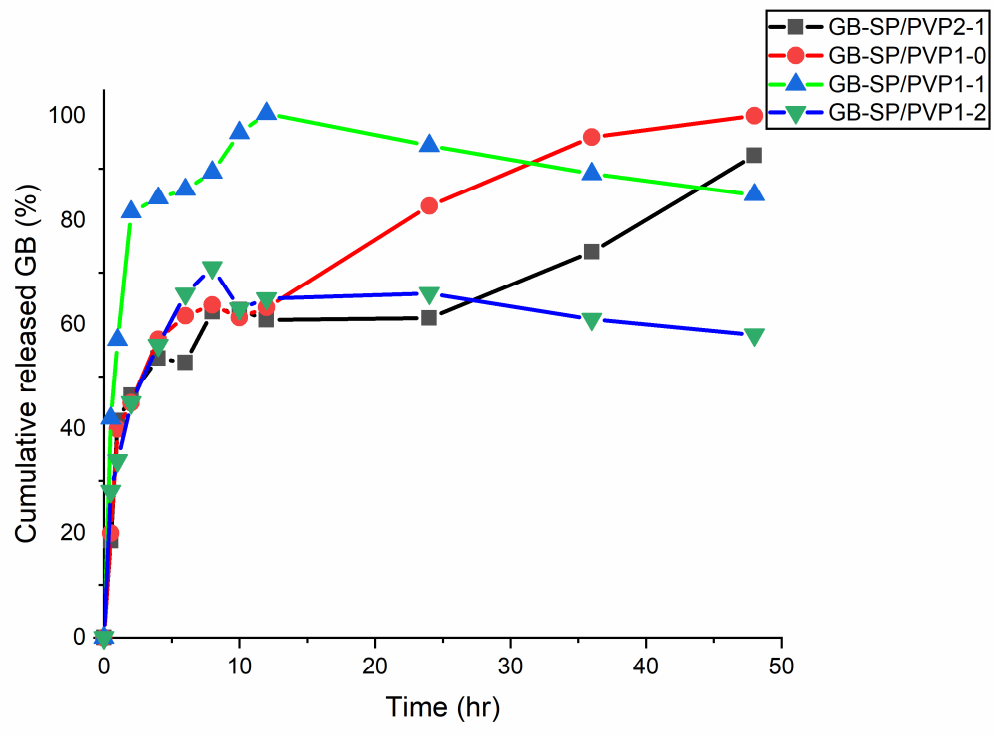
Cumulative released GB (%)
Time (hr)
GB-SP/PVP2-1
GB-SP/PVP1-0
GB-SP/PVP1-1
GB-SP/PVP1-2
0
20
40
60
80
100
0
10
20
30
40
50

Fig. 4. In vitro percentage glibenclamide release from wound dressings of (a) GB-loaded PVP and (b) GB-loaded SP/PVP in different ratios in phosphate buffer PH 7.4 at 37 ºC.

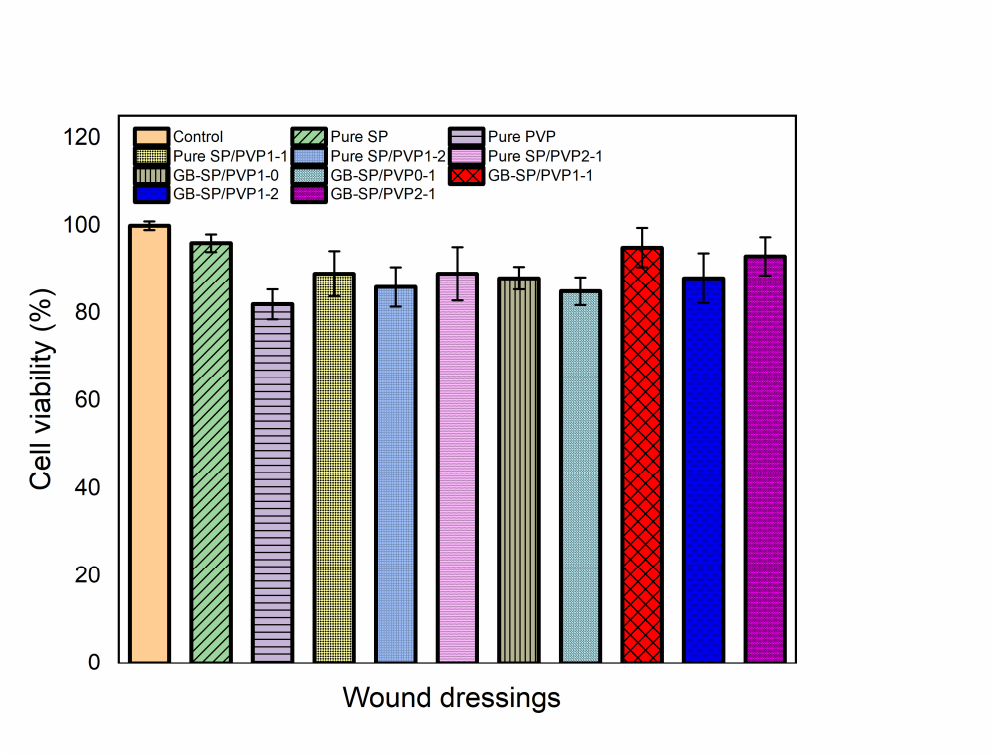

Fig. 5. NIH/3T3 (mouse embryo fibroblast) cell viability of GB-loaded SP/PVP wound dressings over 72 hours. The data are given as average ± standard error of the average.

a

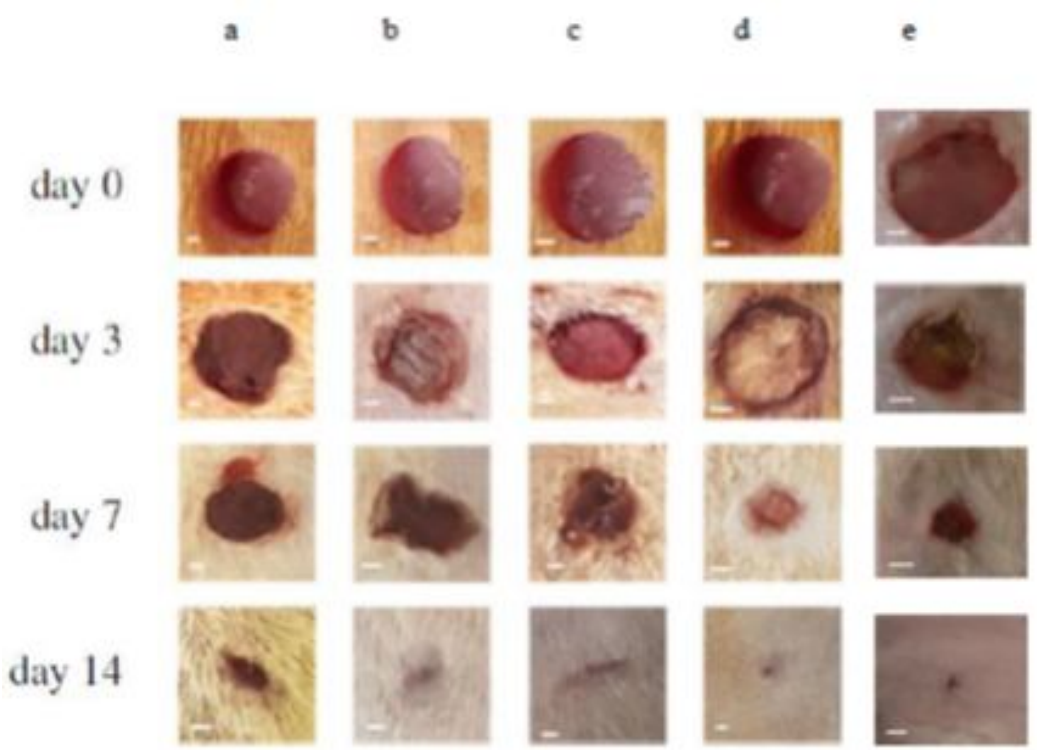
a
b
c
d
e
day 0
day 3
day 7
day 14

b

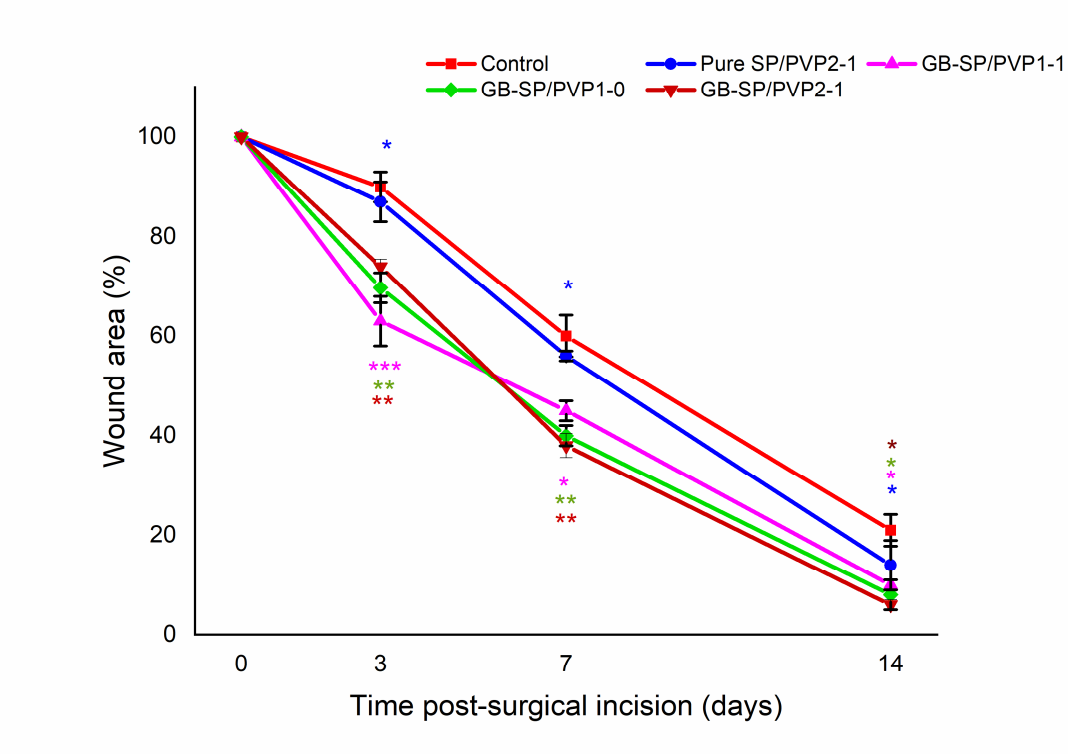
Control
Pure SP/PVP2-1
GB-SP/PVP1-1
GB-SP/PVP1-0
GB-SP/PVP2-1
Wound area (%)
100
80
60
40
20
0
0
3
7
14
Time post-surgical incision (days)

Fig. 6. (a) Illustrative images of wounds from the studied groups: (A) control group, (B) Pure SP/PVP2-1 micelles group, (C) GB-SP/PVP1-1 group, (D) GB-SP/PVP1-0 group, and (E) GB-SP/PVP2-1 group. Scale bar: 1 mm. (b) Percent wound area of diabetic wound as a function of time following different treatment. Data are exhibited as average ± standard error of average. *The symbols *, **, *** represent $p < 0.05$, $p < 0.01$, $p < 0.001$, respectively as compared to control group.*